INSTITUTE OF PHYSICS PUBLISHING INVERSE PROBLEMS

Inverse Problems **18** (2002) 979–1001 PII: S0266-5611(02)33630-X

Optimal finite difference grids for direct and inverse Sturm–Liouville problems

Liliana Borcea[1] **and Vladimir Druskin**[2]

[1] Computational and Applied Mathematics, MS 134, Rice University, 6100 Main Street, Houston, TX 77005-1892, USA
[2] Schlumberger-Doll Research Center, Old Quarry Road, Ridgefield, CT 06877-4108, USA

E-mail: borcea@caam.rice.edu and druskin@sdr.slb.com

Received 8 February 2002, in final form 30 April 2002
Published 27 May 2002
Online at stacks.iop.org/IP/18/979

Abstract

We study finite difference approximations of solutions of direct and inverse Sturm–Liouville problems, in a finite or infinite interval on the real line. The discretization is done on optimal grids, with a three-point finite difference stencil. The optimal location of the grid points is calculated via a rational approximation of the Neumann-to-Dirichlet map and the latter converges exponentially fast. We prove that optimal grids obtained for constant coefficients are asymptotically optimal for variable coefficient direct problems. We also show that optimal grids, together with methods of inverse spectral problems for Jacobi matrices, can be used for the solution of continuous inverse Sturm–Liouville problems. In particular, we formulate and analyse a new inversion algorithm, where the unknown coefficients that we image are optimally discretized. We prove that optimal grids provide necessary conditions for convergence of the discrete inverse problem and we demonstrate the effectiveness of our imaging approach through numerical simulations.

1. Introduction

We consider Sturm–Liouville equations in finite or semi-infinite intervals of the real line, and we let $f(\lambda)$, for some spectral parameter λ, be the Neumann-to-Dirichlet map (also known as the boundary impedance, Poincaré–Steklov operator, Weyl or resolvent function). Sturm–Liouville equations arise in applications such as oscillatory motions of strings, electrical conduction, wave propagation and scattering in layered materials, etc (see section 1.2 for more details).

The objective of this study is twofold:

(a) for direct, variable coefficient Sturm–Liouville problems, we seek optimal finite difference approximations of the Neumann-to-Dirichlet map;

(b) for isotropic, inverse Sturm–Liouville problems, we reconstruct the variable coefficients of the equations, given the Neumann-to-Dirichlet map $f(\lambda)$, for different spectral parameters λ.

The computation of the Neumann-to-Dirichlet map is a principal component of numerical partial differential equation solvers, where it is used for the truncation of computational domains [1, 2], domain decomposition techniques [3, 4], etc. The Neumann-to-Dirichlet map is also known to determine uniquely the coefficients of isotropic, Sturm–Liouville equations [5–7]. Such important applications, in both direct and inverse problems, require efficient and accurate approximations of $f(\lambda)$.

The Neumann-to-Dirichlet map can be efficiently calculated via rational operator approximation [8–10]. However, this approach results in nonlocal operator boundary conditions which destroy the structure and sparsity of the linear systems of equations in finite difference or finite element approximations. Here, we follow the ideas in [11, 12] and we consider finite difference approximations of $f(\lambda)$, where the equations are discretized on k point *optimal* grids. These grids are calculated via the rational approximation of $f(\lambda)$, by $f_k(\lambda)$, the finite difference Neumann-to-Dirichlet map. We consider multi-point Padé approximants of $f(\lambda)$ [13], which is exact at $2k$ points λ_p distributed on a positive bounded spectral interval. The result is that, as $k \to \infty$, $f_k(\lambda)$ converges to $f(\lambda)$ at an *exponential rate*.

Connections between finite difference schemes and Padé approximants have been used before in [14], where it has been shown that the global convergence order is proportional to the size of the stencil. Restrictions of the convergence order by the size of the stencil have also been pointed out for more traditional, adaptive grid methods [15]. The approach considered in this paper and in [11, 12, 16] gives exponential convergence of the solution at the boundary of the domain, without increasing the stencil. The trade-off is the lower accuracy of the solution in the interior of the domain, although, in the limit $k \to \infty$, global convergence is still achieved.

While optimal grids have been applied very successfully to the solution of direct problems [11, 12, 16–18], they have not been used in inversion. Clearly, inverse Sturm–Liouville problems have been the topic of numerous studies and many questions have been answered successfully in works such as [5–7]. Discrete inverse problems of reconstructing particular, structured matrices from their spectral data are also widely studied, as reflected in the extensive linear algebra literature (see the comprehensive review [19]). However, connections between inversion in continuum and discrete settings have remained largely unexplored.

In this paper, we make the connection between discrete and continuum inverse problems by using the *optimal* finite difference approximation of the Neumann-to-Dirichlet map of Sturm–Liouville equations. The case of one-dimensional, constant coefficient direct problems has been analysed in [11, 12, 16]. These results have also been extended, via domain decomposition techniques and tensor-product schemes, to two-dimensional, constant (piecewise constant) coefficient, elliptic and hyperbolic problems [17, 18]. Here, we consider rather general variable coefficient, one-dimensional equations and we demonstrate through analysis and numerical computations that, for such problems, optimal grids are very useful in both *forward modelling* and *inversion*.

The results of this paper can be outlined as follows. Generally, finite difference schemes can be interpreted as resistor networks. The resistors account for the total resistivity of the medium within the finite difference cells and they can be estimated as products of the grid steps and the medium resistivity at the vertices. When solving the one-dimensional inverse problem for resistor networks [20] or, equivalently, for Jacobi matrices [19], one can only find the resistors, or the matrix elements. To image the medium, one needs to know the finite difference grid. We prove that for convergence of the imaging algorithm to the *isotropic*

continuous solution, it is necessary that the grid be close enough to the optimal grid. If one takes quite a different grid, for example, the equidistant one, the discrete inverse problem does not give the true isotropic solution. Indeed, it converges to an equivalent anisotropic model that can be obtained via the coordinate transformation that maps the optimal grids to the equidistant ones. We show experimentally that optimal grids for variable coefficients are close to those for constant coefficients and we prove that the latter remain optimal for the leading term of the WKB asymptotes of variable coefficient forward problems.

1.1. Model problem

Let us consider a two point boundary value problem for the Sturm–Liouville equation

$$\begin{aligned} &\frac{\mathrm{d}}{\mathrm{d}x}\left[\alpha(x)\frac{\mathrm{d}v(x)}{\mathrm{d}x}\right] - \lambda\beta(x)v(x) - \eta(x)v(x) = 0, \qquad \text{for } 0 < x < l, \\ &-\alpha(0)\frac{\mathrm{d}v}{\mathrm{d}x}(0) = 1, \\ &v(l) = 0, \end{aligned} \tag{1.1}$$

with positive, continuously differentiable coefficients $\alpha(x)$ and $\beta(x)$ and bounded, nonnegative coefficient $\eta(x)$. The spectral parameter λ is complex, such that $\operatorname{Re}\sqrt{\lambda} \geqslant 0$ and the size l of the domain can be either finite or infinite. We investigate both direct and inverse problems for the impedance (Neumann-to-Dirichlet) function defined as

$$f(\lambda) = v(0). \tag{1.2}$$

Specifically, in direct problems, we are interested in the accurate numerical approximation of $f(\lambda)$. In inversion, we wish to reconstruct a particular combination of coefficients $\alpha(x)$, $\beta(x)$ and $\eta(x)$, given the impedance $f(\lambda)$ for different spectral parameters λ.

We begin by transforming (1.1) into a simpler, isotropic boundary value problem for a function $u(z)$, defined in the domain $(0, L)$, the image of $(0, l)$ under coordinate stretching

$$z = \int_0^x \sqrt{\frac{\beta(s)}{\alpha(s)}}\,\mathrm{d}s. \tag{1.3}$$

To obtain the new isotropic problem, we define function $g(z) > 0$ as the solution of the Cauchy problem

$$\begin{aligned} &\frac{\mathrm{d}}{\mathrm{d}z}\left[\sqrt{\alpha(z)\beta(z)}\frac{\mathrm{d}g}{\mathrm{d}z}(z)\right] - \eta(z)\sqrt{\frac{\alpha(z)}{\beta(z)}}g(z) = 0, \qquad \text{for } z > 0, \\ &\frac{\mathrm{d}g}{\mathrm{d}z}(0) = 0, \\ &g(0) = 1, \end{aligned} \tag{1.4}$$

and let $u(z) = v(z)/g(z)$. Problem (1.1) is transformed into

$$\begin{aligned} &\frac{\mathrm{d}}{\mathrm{d}z}\left[\sigma(z)\frac{\mathrm{d}u(z)}{\mathrm{d}z}\right] - \lambda\sigma(z)u(z) = 0, \qquad \text{for } 0 < z < L, \\ &-\sigma(0)\frac{\mathrm{d}u(0)}{\mathrm{d}z} = 1, \\ &u(L) = 0, \end{aligned} \tag{1.5}$$

where $\sigma(z) = g^2(z)\sqrt{\alpha(z)\beta(z)}$ is bounded and positive.

Note that with the same coordinate stretch as (1.3) and with the Liouville transformation $w(z) = v(z)h(z)$, where $h(z) = (\alpha(z)\beta(z))^{\frac{1}{4}}$, we obtain from (1.1), Schrödinger's equation

$$\begin{aligned} &\frac{\mathrm{d}^2 w(z)}{\mathrm{d}z^2} - \lambda w(z) - q(z)w(z) = 0, \qquad \text{for } 0 < z < L, \\ &w(0)\frac{\mathrm{d}h}{\mathrm{d}z}(0) - h(0)\frac{\mathrm{d}w}{\mathrm{d}z}(0) = 1, \\ &w(L) = 0, \end{aligned} \tag{1.6}$$

with potential $q(z) = \eta(z)/\beta(z) + \frac{\mathrm{d}^2 h}{\mathrm{d}z^2}(z)/h(z)$. Moreover, as is well known (see for example [21] and section 5.1), equation (1.5) can also be transformed into Schrödinger's equation (1.6), where the potential is given by $q(z) = \frac{\mathrm{d}^2\sqrt{\sigma}}{\mathrm{d}z^2}(z)/\sqrt{\sigma(z)}$.

We study direct and inverse problems for equation (1.5). Explicitly, we consider optimal finite difference approximations of the impedance function of (1.5)

$$f^\sigma(\lambda) = u(0) = v(0) = f(\lambda), \tag{1.7}$$

which is the same as the impedance of (1.1). In inversion, we seek to reconstruct coefficient $\sigma(x)$, for $x \in [0, L]$, given $f^\sigma(\lambda)$, for different values of the spectral parameter λ.

1.2. Motivation

Boundary value problems for Sturm–Liouville equations such as (1.1) and (1.5) arise in many important applications. For example, consider dc electrical conduction in a layered material with electrical conductivity $\sigma(z)$, occupying a strip

$$\Omega = \{(x, y, z) \in \mathbb{R}^3,\ 0 \leqslant z \leqslant L\}.$$

Let us suppose that boundary $z = L$ is grounded and let us take a normal electric current excitation $j(x, y)$ confined to the plane $z = 0$. The electric potential ϕ satisfies

$$\begin{aligned} &\nabla \cdot [\sigma(z)\nabla\phi(x, y, z)] = 0 \qquad \text{in } \Omega, \\ &-\sigma(0)\frac{\partial\phi}{\partial z}(x, y, 0) = j(x, y), \\ &\phi(x, y, L) = 0. \end{aligned}$$

To obtain (1.5), we take the Fourier transform with respect to x and y, and let $\hat{\phi}(\omega_1, \omega_2, z)$, $\hat{j}(\omega_1, \omega_2)$, for $\omega_1, \omega_2 \in \mathbb{R}$, be the Fourier coefficients of ϕ and j, respectively. For fixed frequencies ω_1 and ω_2, we set $\lambda = \omega_1^2 + \omega_2^2 > 0$ and obtain that $u(z) = \frac{\hat{\phi}(\omega_1,\omega_2,z)}{\hat{j}(\omega_1,\omega_2)}$ satisfies (1.5).

A second example considers a wave problem in a time interval $[0, T]$

$$\begin{aligned} &\frac{\partial^2\phi(x,t)}{\partial x^2} - \frac{1}{c^2(x)}\frac{\partial^2\phi(x,t)}{\partial t^2} = 0 \qquad \text{for } 0 < x < l, \\ &-\frac{\partial\phi}{\partial x}(0, t) = r(t), \\ &\phi(l, t) = 0, \\ &\phi(x, 0) = \frac{\partial\phi}{\partial t}(x, 0) = 0, \end{aligned}$$

for a variable wave speed $c(x)$. To obtain (1.1), we write $\phi(x, t)$ and $r(t)$ as time Fourier series, with coefficients $\hat{\phi}(x, \omega)$ and $\hat{r}(\omega)$, respectively, such that $u(x) = \frac{\hat{\phi}(x,\omega)}{\hat{r}(\omega)}$ satisfies (1.1), with $\lambda = -\omega^2 < 0$, $\alpha = 1$, $\beta = 1/c^2(x)$ and $\eta = 0$.

Finally, a third example considers the time-domain Schrödinger equation

$$\begin{aligned}
&\frac{\partial^2\phi(x,t)}{\partial x^2} - q(x)\phi(x,t) - \mathrm{i}\,\frac{\partial\phi(x,t)}{\partial t} = 0 \qquad \text{for } 0 < x < l,\\
&-\frac{\partial\phi}{\partial x}(0,t) = r(t),\\
&\phi(l,t) = 0,\\
&\phi(x,0) = 0,
\end{aligned}$$

with variable potential $q(x)$. Taking the Laplace transform with respect to $t \geqslant 0$, we obtain (1.1) (or (1.6)), with a purely imaginary spectral parameter λ.

1.3. Outline

In section 2 we define and study the properties of optimal grids that give exponential convergence of the finite difference approximation of the boundary impedance of equations (1.1) and (1.5). The global convergence of the finite difference scheme on optimal grids is proven in section 3. The inverse problem is studied in section 4. We show that grids which are optimal for constant coefficients can be efficiently used for the solution of the variable coefficient inverse problem. We formulate an inversion algorithm, we give the necessary conditions for its convergence and we assess its performance through numerical simulations. In section 5, we analyse the accuracy of the finite difference scheme for direct problem (1.5), at high frequency λ. It is at such frequencies that solutions of (1.5) are most singular and therefore most difficult to approximate. We show that optimal grids for constant coefficients give very good accuracy of the finite difference approximation of variable coefficient impedance $f^\sigma(\lambda)$, for $|\lambda| \gg 1$. This is, in fact, a partial motivation for the imaging algorithm introduced in section 4. Conclusions are given in section 6.

2. Optimal finite difference grids

2.1. Formulation of the finite difference problem

We consider a finite difference solution of problem (1.5), on a staggered grid. The numerical approximation of $u(z_j)$, denoted by U_j, is defined at the primary nodes z_j, $j = 1, 2 \ldots k+1$, where $z_1 = 0$ and $h_j = z_{j+1} - z_j > 0$. U_j satisfies

$$\begin{aligned}
&\frac{1}{\hat{h}_j}\left[\hat{\sigma}_j\left(\frac{U_{j+1}-U_j}{h_j}\right) - \hat{\sigma}_{j-1}\left(\frac{U_j - U_{j-1}}{h_{j-1}}\right)\right] - \lambda\sigma_j U_j = 0, \qquad j = 2, 3 \ldots k,\\
&\hat{\sigma}_1\left(\frac{U_2 - U_1}{h_1}\right) - \lambda\hat{h}_1\sigma_1 U_1 = -1,\\
&U_{k+1} = 0,
\end{aligned} \tag{2.8}$$

(see also (2.11)). The finite difference derivatives are defined at the dual nodes $\hat{z}_j$, $j = 0, 1 \ldots k$, where $\hat{z}_0 = 0$ and $\hat{h}_j = \hat{z}_j - \hat{z}_{j-1} > 0$. Coefficients σ_j and $\hat{\sigma}_j$ are approximations of $\sigma(z_j)$ and $\sigma(\hat{z}_j)$, respectively. In the case of discontinuous $\sigma(z)$, σ_j and $\hat{\sigma}_j$ are arithmetic and harmonic averages of $\sigma(z)$, around the grid points z_j and $\hat{z}_j$, respectively. We give a precise definition of these coefficients in section 2.3.

Let us denote by

$$f_k^\sigma(\lambda) = U_1, \tag{2.9}$$

the numerical approximation of the impedance function $f^\sigma(\lambda)$ defined in (1.7). We consider the following problems:

(a) the direct problem of approximating $f^\sigma(\lambda)$ by the finite difference approximation $f_k^\sigma(\lambda)$, for λ in some spectral interval of the real axis;
(b) the inverse problem of determining a positive function $\sigma(z)$, which belongs to a set which is compactly embedded in $L^\infty([0, L])$, given the impedance $f_k^\sigma(\lambda_j)$, for noncoinciding λ_j, $j = 1, 2 \dots 2k$.

In standard finite difference schemes, the mesh points z_j and $\hat{z}_j$, for $j = 1, 2 \dots k$, are related for example by $\hat{z}_j = (z_j + z_{j+1})/2$ and the accuracy of the approximation of $f^\sigma(\lambda)$, by $f_k^\sigma(\lambda)$, is second order in the mesh size. We consider instead grids where h_j and $\hat{h}_j$, for $j = 1, 2 \dots k$, are independent, positive variables. Among all such grids, we are interested in optimal ones, where $f_k^\sigma(\lambda)$ converges to $f^\sigma(\lambda)$ exponentially, as k increases.

2.2. *Rational representation of the discrete impedance*

Let us define the positive coefficients

$$\gamma_j = \frac{h_j}{\hat{\sigma}_j}, \qquad \hat{\gamma}_j = \hat{h}_j \sigma_j, \qquad \text{for } j = 1, 2 \dots k, \tag{2.10}$$

and let us extend the solution of (2.8) to a dummy node $z_0 = z_1 - h_0$, for a very small h_0, in such a way that

$$-\sigma(0)\frac{U_1 - U_0}{h_0} = -\sigma(0)\frac{\mathrm{d}u}{\mathrm{d}z}(0) = 1. \tag{2.11}$$

Then, if we let $\gamma_0 = h_0/\sigma(0)$, (2.8) becomes

$$\begin{aligned} &\frac{1}{\hat{\gamma}_j}\left(\frac{U_{j+1} - U_j}{\gamma_j} - \frac{U_j - U_{j-1}}{\gamma_{j-1}}\right) - \lambda U_j = 0, \qquad \text{for } j = 1, 2 \dots k, \\ &U_{k+1} = 0, \end{aligned} \tag{2.12}$$

or, in short, writing the discrete difference operator as a tridiagonal, $k \times k$ matrix Δ_γ, we have

$$(\Delta_\gamma - \lambda I)\boldsymbol{U} = -\frac{1}{\hat{\gamma}_1}\boldsymbol{e}_1, \tag{2.13}$$

where $\boldsymbol{U} = (U_1, U_2 \dots U_k)^T$, I is the $k \times k$ identity matrix and $\boldsymbol{e}_1$ is the unit vector in $\mathbb{R}^k$, with all but the first components equal to zero.

Note that Δ_γ is symmetric with respect to weighted inner product

$$\langle \boldsymbol{a}, \boldsymbol{b} \rangle_{\hat{\gamma}} = \sum_{p=1}^{k} a_p b_p \hat{\gamma}_p, \qquad \text{for } \boldsymbol{a} = (a_1, \dots, a_k)^T \text{ and } \boldsymbol{b} = (b_1, \dots, b_k)^T \in \mathbb{R}^k \tag{2.14}$$

and

$$\langle \boldsymbol{a}, \Delta_\gamma \boldsymbol{a} \rangle_{\hat{\gamma}} < 0, \qquad \text{for all } \boldsymbol{a} \in \mathbb{R}^k, \boldsymbol{a} \neq 0. \tag{2.15}$$

In fact, $\mathrm{diag}(\hat{\gamma}_1, \dots, \hat{\gamma}_k)\Delta_\gamma$ is a Jacobi matrix. Therefore, Δ_γ has k orthonormal (with respect to inner product (2.14)) eigenvectors $\boldsymbol{X}^{(1)}, \dots, \boldsymbol{X}^{(k)}$ and simple, negative eigenvalues $\theta^{(k)}$, which we order as

$$\theta^{(k)} < \theta^{(k-1)} < \cdots < \theta^{(1)} < 0,$$

such that, in the limit $k \to \infty$, $\theta^{(k)} \to -\infty$ (see also lemma 4).

We write the solution $\boldsymbol{U}$ of (2.13) as a linear combination of the eigenvectors of Δ_γ and obtain the following representation of $f_k^\sigma(\lambda)$.

Lemma 1. *The discrete impedance function (2.9) is given in terms of the eigenvalues $\theta^{(p)}$ and the first components of the eigenvectors $X_1^{(p)}$, for $p = 1, \ldots k$, as*

$$f_k^\sigma(\lambda) = \sum_{p=1}^{k} \frac{y_p}{\lambda - \theta^{(p)}}, \tag{2.16}$$

where $y_p = (X_1^{(p)})^2$.

For a proof, see [11, 17]. Thus, $f_k^\sigma(\lambda)$ is a Markov function with discrete measure μ_k, which has k points of increase located at $\theta^{(j)}$, where weights y_p are concentrated, for $1 \leqslant j \leqslant k$.

It is known that a rational function such as (2.16) can also be written as a finite continued fraction [13, 22]. Such a representation of $f_k^\sigma(\lambda)$ can be understood by interpreting the solution U_j of (2.12) as the transversal displacement of a point mass $\hat{\gamma}_j$, located at coordinate $\sum_{i=1}^{j-1} \gamma_j$ along a discrete Stieljes string, oscillating at frequency $\sqrt{\lambda}$, for $j = 1, \ldots, k$ [23].

Lemma 2. *The discrete impedance function (2.9) has the finite continued fraction representation*

$$f_k^\sigma(\lambda) = \cfrac{1}{\hat{\gamma}_1\lambda + \cfrac{1}{\gamma_1 + \cfrac{1}{\hat{\gamma}_2\lambda + \cdots \cfrac{1}{\gamma_{k-1} + \cfrac{1}{\hat{\gamma}_k\lambda + \cfrac{1}{\gamma_k}}}}}}. \tag{2.17}$$

The representation (2.17) is unique and there is an explicit relationship between the coefficients in (2.17) and the moments of discrete measure μ_k

$$s_n = \sum_{p=1}^{k} y_p |\theta^{(p)}|^n, \qquad \text{for } n = 0, 1, 2, \ldots. \tag{2.18}$$

Lemma 3. *The coefficients in (2.17) are given by*

$$\frac{\hat{\gamma}_j}{\hat{\gamma}_1} = \frac{B_{j-1}^2}{A_j A_{j-1}}, \qquad \textit{and} \qquad \hat{\gamma}_1\gamma_j = \frac{A_j^2}{B_j B_{j-1}}, \qquad \textit{for } j = 1, 2, \ldots k, \tag{2.19}$$

where A_j and B_j are the strictly positive determinants

$$A_j = \begin{vmatrix} s_0 & s_1 & \ldots & s_{j-1} \\ s_1 & s_2 & \ldots & s_j \\ \vdots & \vdots & & \vdots \\ s_{j-1} & s_j & \ldots & s_{2j-2} \end{vmatrix},$$

$$B_j = \begin{vmatrix} s_1 & s_2 & \ldots & s_j \\ s_2 & s_3 & \ldots & s_{j+1} \\ \vdots & \vdots & & \vdots \\ s_j & s_{j+1} & \ldots & s_{2j-1} \end{vmatrix}, \qquad \textit{for } j \geqslant 1, A_0 = B_0 = 1, \tag{2.20}$$

and

$$\hat{\gamma}_1 = 1 \Big/ \sum_{p=1}^{k} y_p. \tag{2.21}$$

Note that sequence $\{s_j\}_{j\geqslant 0}$ is positive definite since, for $n \leqslant k-1$,

$$\sum_{i,j=0}^{n-1} s_{i+j+m}\zeta_i\zeta_j = \sum_{p=1}^{k} y_p|\theta^{(p)}|^m\left(\sum_{j=0}^{n-1}\zeta_j|\theta^{(p)}|^j\right)^2 > 0, \qquad \text{for all } (\zeta_0,\dots\zeta_{n-1}) \neq 0. \quad (2.22)$$

Therefore, if we let $m = 0$ or 1 in (2.22), we obtain that $A_n > 0$ and $B_n > 0$, for all $n \geqslant 0$. Stieljes has shown that having determinants A_n and B_n strictly positive is the necessary and sufficient condition that $f_k^{\sigma}(\lambda)$ be given by (2.17), with coefficients (2.19). The proof of (2.19) is given in [23]. Furthermore, since the eigenvectors are orthonormal with respect to inner product (2.14), matrix

$$V = \operatorname{diag}(\hat{\gamma}_1^{\frac{1}{2}}, \hat{\gamma}_2^{\frac{1}{2}}, \dots, \hat{\gamma}_k^{\frac{1}{2}})(\boldsymbol{X}^{(1)}, \boldsymbol{X}^{(2)}, \dots, \boldsymbol{X}^{(k)})$$

is orthogonal and

$$\sum_{p=1}^{k} V_{1p}^2 = \hat{\gamma}_1 \sum_{p=1}^{k}(X_1^{(p)})^2 = \hat{\gamma}_1 \sum_{p=1}^{k} y_p = 1. \quad (2.23)$$

We finally note that the recovery of γ_j and $\hat{\gamma}_j$, from y_p and $\theta^{(p)}$, for j, $p = 1, 2\dots, k$, as given in lemma 3, is equivalent to solving the discrete inverse eigenvalue problem:
Find the symmetric (with respect to inner product (2.14)) tridiagonal matrix Δ_γ, *with eigenvalues* $\theta^{(p)} < 0$ *and first components of the eigenvectors satisfying* $y_p = (X_1^{(p)})^2 > 0$, *for* $p = 1, \dots, k$.
This problem is known to have a unique solution (see for example [19]) and it is commonly solved using the Lanczos method.

2.3. Definition of the optimal grid

Let us introduce the coordinate transformation

$$x(z) = \int_0^z \frac{\mathrm{d}s}{\sigma(s)}, \quad (2.24)$$

and take the monotone increasing map

$$M : [0, x(L)] \to [0, \hat{x}(L)], \qquad M(x(z)) = \hat{x}(z) = \int_0^z \sigma(s)\,\mathrm{d}s. \quad (2.25)$$

The boundary value problem (1.5) can be rewritten as

$$\begin{aligned} &\frac{\mathrm{d}}{\mathrm{d}M(x)}\left[\frac{\mathrm{d}u(x)}{\mathrm{d}x}\right] - \lambda u(x) = 0, \qquad \text{for } 0 < x < l \leqslant \infty, \\ &-\frac{\mathrm{d}u(0)}{\mathrm{d}x} = 1, \\ &u(l) = 0, \end{aligned} \quad (2.26)$$

and it describes the motion of a string with a fixed right end point, oscillating at frequency $\sqrt{\lambda}$, under a Neumann boundary excitation at the left end point. At coordinate x along the string, the mass distribution is given by $M(x)$. The length of the string is $l = x(L)$ and its total mass is $M(l) = \hat{x}(L)$.

The impedance functions of such strings are completely characterized in [23]. In particular, it is shown in [23] that $f^{\sigma}(\lambda)$ has the following representation.

Lemma 4. *The impedance $f^\sigma(\lambda)$ of (1.5) is a Stieljes function, written in terms of its spectral measure μ, as*

$$f^\sigma(\lambda) = \int_{-\infty}^{0} \frac{\mathrm{d}\mu(s)}{\lambda - s}. \tag{2.27}$$

If the length L of the interval in (1.5) is finite, measure μ is discrete and $f^\sigma(\lambda)$ has an infinite number of distinct, negative poles ξ_n and positive residues r_n, for $n \geqslant 1$. Moreover, as $n \to \infty$, $\xi_n \to -\infty$ in such a way that

$$\lim_{n\to\infty} \frac{n}{\sqrt{|\xi_n|}} = \frac{1}{\pi}\int_0^L \sigma(s)\,\mathrm{d}s.$$

If the length L of the interval is infinite, the spectrum of measure μ is continuous.

It is clear that impedance $f_k^\sigma(\lambda)$ is completely determined by coefficients (2.10), so we write

$$f_k^\sigma \equiv f_k^\Gamma, \qquad \text{where } \Gamma = \{\gamma_j, \hat{\gamma}_j, \text{ for } 1 \leqslant j \leqslant k\}. \tag{2.28}$$

The optimal accuracy of f_k^σ can be obtained by minimizing over all parameters γ_j and $\hat{\gamma}_j$

$$\max_{\lambda\in[\Lambda_1,\Lambda_2]} |f_k^\Gamma(\lambda) - f^\sigma(\lambda)|,$$

for some interval $[\Lambda_1, \Lambda_2]$ chosen from *a priori* information about the spectral properties of the solution. There are a few cases of known analytical and asymptotic solutions of such a minimization problem [12] but, in general, rational minimization is notoriously difficult. However, we can take a simpler approach, where we select $2k$ noncoinciding interpolation points λ_p in the spectral interval and we let

$$f_k^\Gamma(\lambda_p) = f^\sigma(\lambda_p), \qquad \text{for } 1 \leqslant p \leqslant 2k. \tag{2.29}$$

Of course, it is desirable to pick λ_p close to the interpolation points of the optimal approximation. Nevertheless, just taking them anywhere, within a bounded spectral interval $[\Lambda_1, \Lambda_2]$, yields exponential convergence for all λ outside the poles of f^σ [11, 13, 22]. In the limit case, when all λ_p converge to one point, we obtain a simple Padé approximant [13] which also converges exponentially, but at a rate that deteriorates rapidly away from the matching point. The multi-point Padé algorithm for (2.29) gives a unique solution f_k^Γ, of the form (2.16), with positive y_p and negative, distinct $\theta^{(p)}$, for $1 \leqslant p \leqslant k$, as shown in [13].[1] We call the grids given by (2.29) and the corresponding $2k$ parameters γ_j and $\hat{\gamma}_j$ (see lemma 3), the optimal grids, although they are truly optimal just for the interpolation points λ_p.

Note that, in (2.29), $f^\sigma(\lambda_p)$ is either measured (in inverse problems) or it is calculated numerically, on a very fine grid (in forward problems), for the desired $2k$ spectral parameters λ_p.

In the direct problem, function $\sigma(z)$ is known for all $z \in [0, L]$ and, given the coefficients (2.10), we can easily determine the grid points. For example, in case of continuous $\sigma(z)$, we can use the algorithm:

Algorithm 1. *For $j = 1, 2 \ldots, k$, calculate the grid points as*

$$\hat{h}_j = \tfrac{\hat{\gamma}_j}{\sigma(z_j)}, \qquad \hat{z}_j = \hat{z}_{j-1} + \hat{h}_j, \qquad \textit{where } \hat{z}_0 = 0,$$
$$h_j = \sigma(\hat{z}_j)\gamma_j, \qquad z_{j+1} = z_j + h_j, \qquad \textit{where } z_1 = 0.$$

We prefer instead a more general construction of the grid, which also allows discontinuous $\sigma(z)$.

[1] A simple and efficient modification of such an approach is the Padé–Chebyshev approximant, which requires that the first $2k$ Chebyshev coefficients of the continuum and discrete impedances match [11, 13, 22]. The approximation also has an equivalent formulation as a Stieljes moment problem [13, 22].

Figure 1. Optimal grid, $k = 20$, $L = 1$, the dots are the primary points z_i and the crosses are the dual points $\hat{z}_i$.

Algorithm 2. *Find* $\hat{z_j}$ *and* z_{j+1} *from equations* $\int_0^{\hat{z}_j} \sigma(z)\,\mathrm{d}z = \sum_{p=1}^{j} \hat{\gamma}_p$, *and* $\int_0^{z_{j+1}} \frac{\mathrm{d}z}{\sigma(z)} = \sum_{p=1}^{j} \gamma_p$, *respectively, where* $j = 1, 2 \ldots, k$ *and* $\hat{z}_0 = z_1 = 0$.

Note that, since γ_p, $\hat{\gamma}_p$ and $\sigma(z)$ are positive and bounded, algorithm 2 generates grid points

$$0 = z_1 < z_2 < z_3 < \cdots < z_{k+1},$$
$$0 = \hat{z}_0 < \hat{z}_1 < \hat{z}_2 < \cdots < \hat{z}_k,$$

which we conjecture, based on extensive numerical experiments [11, 12, 16, 18], are interlaced as

$$0 = \hat{z}_0 = z_1 < \hat{z}_1 < z_2 < \hat{z}_2 < z_3 < \cdots < \hat{z}_k < z_{k+1}. \tag{2.30}$$

Note also that algorithm 2, combined with (2.10), gives

$$\frac{1}{\hat{\sigma}_j} = \frac{1}{h_j}\int_{z_j}^{z_{j+1}} \frac{\mathrm{d}z}{\sigma(z)}, \qquad \sigma_j = \frac{1}{\hat{h}_j}\int_{\hat{z}_{j-1}}^{\hat{z}_j} \sigma(z)\,\mathrm{d}z, \qquad \text{for } j = 1, 2 \ldots k, \tag{2.31}$$

so that $\hat{\sigma}_j$ and σ_j in discretization (2.8) are the harmonic and arithmetic means of $\sigma(z)$, in intervals (z_j, z_{j+1}) and $(\hat{z}_{j-1}, \hat{z}_j)$, respectively.

2.4. Properties of optimal grids

We refer to the grid defined in section 2.3 as the optimal grid because the finite difference impedance $f_k^{\Gamma}(\lambda)$ converges exponentially, as k increases, to $f^{\sigma}(\lambda)$, for $\lambda \in [\Lambda_1, \Lambda_2]$. In fact, the approximation of the impedance is not very sensitive to the spectral interval $[\Lambda_1, \Lambda_2]$, and the convergence remains exponential (with a lower decay rate) even for $\lambda \notin [\Lambda_1, \Lambda_2]$ [11].

The distribution of the grid points in the interior of the domain depends strongly on the Padé interpolation points $\lambda_p \in [\Lambda_1, \Lambda_2]$. However, common features (experimentally observed but not yet rigorously explained) of all optimal grids, with respect to various interpolation points λ_p, are the gradual refinement near the point $z = 0$ of measurements and the alternation property (2.30) (see for example figure 1). Moreover, as we increase k, the end point z_{k+1} approaches L at an exponential rate and the optimal grids fill the domain $[0, L]$, as given in the following proposition.

Proposition 1. *On the optimal grid, we have, as* $k \to \infty$,

$$\sum_{j=1}^{k} \gamma_j = \sum_{j=1}^{k} \frac{h_j}{\hat{\sigma}_j} = \int_0^{z_{k+1}} \frac{\mathrm{d}z}{\sigma(z)} \longrightarrow \int_0^{L} \frac{\mathrm{d}z}{\sigma(z)}, \tag{2.32}$$

where the convergence rate is exponential in k. *Then,* z_{k+1} *converges to* L, *exponentially in* k.

Proof. From the continued fraction representation of $f_k^{\Gamma}(\lambda)$ (see lemma 2) and from algorithm 2, we have for $\lambda = 0$,

$$f_k^{\Gamma}(0) = \sum_{j=1}^{k} \gamma_j = \int_0^{z_{k+1}} \frac{\mathrm{d}z}{\sigma(z)}.$$

The impedance $f^\sigma(0)$ of continuum problem (1.5) is

$$f^\sigma(0) = \int_0^L \frac{\mathrm{d}z}{\sigma(z)}$$

and, by the optimality of the grid, in the limit $k \to \infty$, we obtain (2.32). In the simple case of constant σ, the exponential convergence of z_{k+1} to L follows trivially from (2.32). When σ varies with z, (2.32) gives $\int_{z_{k+1}}^L \frac{\mathrm{d}z}{\sigma(z)} \to 0$. Since σ is a positive, bounded function, $z_{k+1} \to L$, exponentially fast in k.

To give our final note on the properties of optimal grids, let us introduce the discrete coordinate transformation

$$x_{j+1} = \sum_{i=1}^{j} \gamma_i \qquad \text{and} \qquad \hat{x}_j = \sum_{i=1}^{j} \hat{\gamma}_i, \qquad \text{for } 1 \leqslant j \leqslant k, \text{ where } x_1 = \hat{x}_0 = 0, \quad (2.33)$$

and take a piecewise constant, monotone increasing map

$$M_k(x) = \hat{x}_j, \qquad \text{if } x \in [x_j, x_{j+1}), \qquad \text{for } 1 \leqslant j \leqslant k. \quad (2.34)$$

Note that (2.33) and (2.34) are the discrete equivalents of (2.24) and (2.25) and they have the physical meaning of coordinate along the string and mass distribution, respectively. □

We have the following convergence result for the optimal grid points.

Proposition 2. *As $k \to \infty$, h_j and $\hat{h}_j \to 0$ and, furthermore, primary grid points z_j converge to dual points $\hat{z}_j$, for all $1 \leqslant j < \infty$.*

Proof. Consider the sequence $\{M_k(x)\}$ of mass distributions of the Stieljes string. Recall that each function in the sequence is positive, monotonically increasing and bounded over a finite interval. Hence, by Helley's selection theorem (see [24]), there exists a subsequence, which we denote by $\{M_k(x)\}$ as well, which converges pointwise in a finite interval, to a function $\mathcal{M}(x)$. However, by construction, the impedance $f_k^\Gamma(\lambda)$ of the Stieljes string with mass distribution $M_k(x)$ converges at an exponential rate to $f^\sigma(\lambda)$, the impedance of the Stieljes string with continuous mass distribution $M(x)$ (see (2.25)). Thus, due to the uniqueness of solution of the inverse problem, we have that limit function $\mathcal{M}(x) = M(x)$. Furthermore, since each $M_k(x)$ is a piecewise constant function over intervals of length $x_{i+1} - x_i = \gamma_i$, and since the limit function is continuous, we have $\lim_{k\to\infty} \gamma_i = 0$. In particular, since σ is bounded and strictly positive, $h_i \to 0$. Now, by definition of the grid (see algorithm 2), we have $x_j = x(z_j)$ and $\hat{x}_j = \hat{x}(\hat{z}_j)$, for all $j = 1, \ldots, k$. But (2.34) gives that $M_k(x_j) = \hat{x}_j = M(x(\hat{z}_j))$ and, since $M_k \to M$, we have $x_j = x(z_j) \to x(\hat{z}_j)$. However, function $x(z)$ is strictly monotone, which means that $z_j \to \hat{z}_j$. □

3. Global convergence of the finite difference solution

Let us denote by $E_j = U_j - u(z_j)$ the error of finite difference problem (2.12), and by T_j the truncation error

$$\begin{aligned} T_j &= \frac{1}{\hat{\gamma}_j}\left(\frac{u(z_{j+1}) - u(z_j)}{\gamma_j} - \frac{u(z_j) - u(z_{j-1})}{\gamma_{j-1}}\right) - \lambda u(z_j) \\ &= \frac{\mathrm{d}u}{\mathrm{d}z}(z_j)\left(\frac{\hat{\sigma}_j - \hat{\sigma}_{j-1}}{\hat{h}_j \sigma_j} - \frac{1}{\sigma(z_j)}\frac{\mathrm{d}\sigma}{\mathrm{d}z}(z_j)\right) + \frac{\mathrm{d}^2u}{\mathrm{d}z^2}(z_j)\left(\frac{\hat{\sigma}_j h_j + \hat{\sigma}_{j-1} h_{j-1}}{2\hat{h}_j \sigma_j} - 1\right) \\ &\quad + \frac{1}{6\hat{h}_j \sigma_j}\left[\hat{\sigma}_j h_j^2 \frac{\mathrm{d}^3u}{\mathrm{d}z^3}(\zeta_j) - \hat{\sigma}_{j-1} h_{j-1}^2 \frac{\mathrm{d}^3u}{\mathrm{d}z^2}(\zeta_{j-1})\right], \end{aligned} \quad (3.35)$$

where ζ_j is some point in (z_j, z_{j+1}), for $j = 1, 2, \ldots, k$. We have the following global error estimate for the finite difference solution on the optimal grid.

Theorem 1. *For any given k and for all spectral parameters λ that are not eigenvalues of the discrete operator Δ_γ, the error at all grid points is uniformly bounded in terms of the truncation error. Moreover, as $k \to \infty$, $E_j \to 0$, for all $1 \leqslant j \leqslant k+1$, and at the end points z_1 and z_{k+1}, the convergence is exponential.*

Proof. By the construction of the optimal grid, $E_1 \to 0$, exponentially in k. At z_{k+1}, the error is $E_{k+1} = -u(z_{k+1})$ and, by proposition 1, $z_{k+1} \to L$, exponentially in k, so $E_{k+1} \to 0$, exponentially fast, as well. To obtain the error at the interior points, we begin with the error equation

$$(\lambda I - \Delta_\gamma)\boldsymbol{E} = \boldsymbol{T} - \left(\frac{E_1 - E_0}{\gamma_0}\right)\frac{\boldsymbol{e}_1}{\hat{\gamma}_1}, \tag{3.36}$$

where $\boldsymbol{E} = (E_1, E_2 \ldots E_k)^T$, $\boldsymbol{T} = (T_1, \ldots, T_k)^T$ and where, by (2.11), we have

$$\delta = \frac{E_1 - E_0}{\gamma_0} = \sigma(0)\left(\frac{U_1 - U_0}{h_0} - \frac{u(z_1) - u(z_0)}{h_0}\right) = \sigma(0)\frac{h_0}{2}\frac{\mathrm{d}^2 u}{\mathrm{d}z^2}(\xi) = \lambda\sigma(0)u(\xi)\frac{h_0}{2}, \tag{3.37}$$

for some $\xi \in (z_0, z_1)$. Next, we write $\boldsymbol{E}$ as a linear combination of the eigenvectors of Δ_γ, and obtain

$$E_j = \sum_{p=1}^{k} \frac{X_j^{(p)}}{\lambda - \theta^{(p)}}[\langle \boldsymbol{T}, \boldsymbol{X}^{(p)}\rangle_{\hat{\gamma}} + X_1^{(p)}\delta], \qquad \text{for } j = 1, 2 \ldots k, \tag{3.38}$$

where, by (2.10),

$$\langle \boldsymbol{T}, \boldsymbol{X}^{(p)}\rangle_{\hat{\gamma}} = \sum_{j=1}^{k} \hat{h}_j \sigma_j T_j X_j^{(p)}.$$

□

Clearly, δ is proportional to h_0, which can be chosen to be arbitrarily small. Therefore, if $\lambda \neq \theta^{(p)}$, for $p = 1, 2 \ldots k$, the error at the interior points is essentially bounded in terms of the truncation error. Moreover, due to proposition 2, as $k \to \infty$, the truncation error (3.35) decays to zero and global convergence of the finite difference solution follows.

4. Imaging on optimal grids

In this section, we consider the inverse problem of determining coefficient $\sigma \in \mathcal{S}$ in equation (1.5), where $\mathcal{S}$ is a compact set of bounded, positive functions. We solve the inverse problem by considering the finite difference scheme (2.8) and the impedance data $f^\sigma(\lambda_i^k)$ for a set $\mathcal{L}_k$ of noncoinciding spectral parameters λ_i^k, $i = 1, 2 \ldots 2k$.

Obviously, the finite difference impedance (2.28) depends only on parameters γ_i and $\hat{\gamma}_i$, for $i = 1, 2 \ldots k$, which are uniquely determined by the system of equations

$$f_k^\Gamma(\lambda_i^k) = f^\sigma(\lambda_i^k), \qquad \text{for } 1 \leqslant i \leqslant 2k. \tag{4.39}$$

Let us consider a sequence of sets $\mathcal{L}_k$, such that $\lim_{k\to\infty} f_k^\Gamma(\lambda) = f^\sigma(\lambda)$, where the convergence is at an exponential rate, for all complex $\lambda \in \mathcal{L}_k$, except the poles of f^σ. In fact, there is global convergence of the solution of the finite difference problem (2.12) (see theorem 1), although the exponential rate occurs only at the end points of interval $[0, L]$.

Thus, it is reasonable to expect that the solution of the continuous inverse problem $\sigma(z)$ is the limit of solutions $\sigma^k(z)$ of the discrete inverse problems. Note however that from the data (equations (4.39)), we can only find coefficients γ_i and $\hat{\gamma}_i$, for $i = 1, 2 \ldots k$. In order to find $\sigma^k(z)$, we must define the grid.

Our objective is to find, out of the infinitely many choices, those grids that give convergence of the solution of the discrete inverse problem, to the solution of the continuum inverse problem, for all functions $\sigma \in \mathcal{S}$. More precisely, we seek grids which are dependent on the spectral parameters in $\mathcal{L}_k$, but independent of $\sigma(z)$, such that

$$\max_{\sigma\in\mathcal{S}} \left| \int_0^{\hat{z}_i} \sigma(z)\,\mathrm{d}z - \sum_{j=1}^{i} \hat{\gamma}_j \right| < \epsilon_k, \qquad \text{for } i = 1, \ldots, k+1,$$

$$\max_{\sigma\in\mathcal{S}} \left| \int_0^{z_{i+1}} \frac{1}{\sigma(z)}\,\mathrm{d}z - \sum_{j=1}^{i} \gamma_j \right| < \epsilon_k, \qquad \text{for } i = 1, \ldots, k, \tag{4.40}$$

where $\epsilon_k > 0$ and $\lim_{k\to\infty} \epsilon_k = 0$. If (4.40) holds and such grids exist, then grid conductivities $\hat{\sigma}_i$ and σ_i converge to the harmonic and arithmetic means of true $\sigma(z)$, over intervals (z_i, z_{i+1}) and $(\hat{z}_{i-1}, \hat{z}_i)$, respectively, for $i = 1, \ldots, k$.

Clearly, the question of the existence of such grids depends on the set $\mathcal{S}$ of conductivities. However, we can expect, and the numerical experiments confirm this, that if $\mathcal{S}$ consists of functions $\sigma(z)$ which are 'sufficiently similar' to each other, such grids can be found. A more precise statement is:

Proposition 3. *Given a compact set $\mathcal{S}$ of bounded, positive functions, let us denote by $\mathcal{G}_k^\sigma$, the optimal grid corresponding to function $\sigma \in \mathcal{S}$ and a given set $\mathcal{L}_k$ of noncoinciding spectral points. The following two statements are equivalent:*

(a) For a given set $\mathcal{L}_k$ of spectral points, the optimal grids $\mathcal{G}_k^\sigma$ obtained with the help of algorithm 2, for all $\sigma \in \mathcal{S}$, are asymptotically close, in the limit $k \gg 1$.
(b) Let $\tilde{\sigma}^k(z)$ be the solution of the discrete inverse problem, obtained with grid $\mathcal{G}_k^{\sigma^{(0)}}$, for a given, known $\sigma^{(0)} \in \mathcal{S}$. As $k \to \infty$, $\tilde{\sigma}^k(z)$ converges to $\sigma(z)$, the solution of the continuous inverse problem in the sense of (4.40).

Proof. Here, we use the notations z_i^σ and $\hat{z}_i^\sigma$ for the optimal grid in algorithm 2, and $z_i^{\sigma^{(0)}}$ and $\hat{z}_i^{\sigma^{(0)}}$ for the grid in (4.40). If statement (a) holds, we have that, for large enough k,

$$|z_i^{\sigma^{(0)}} - z_i^\sigma| < \sigma(\xi_i)\epsilon_k \qquad \text{and} \qquad |\hat{z}_i^{\sigma^{(0)}} - \hat{z}_i^\sigma| < \frac{\epsilon_k}{\sigma(\hat{\xi}_i)},$$

for some ξ_i between z_i^σ and $z_i^{\sigma^{(0)}}$ and $\hat{\xi}_i$ between $\hat{z}_i^\sigma$ and $\hat{z}_i^{\sigma^{(0)}}$, respectively, so that (4.40) follows from algorithm 2. Next, let us suppose that statement (b) is true. Then, (4.40) and the corresponding equations of algorithm 2 differ only by small terms ϵ_k. Due to the properties of S, the latter equations have a unique and stable solution, so statement (a) follows. □

Remark 1. The asymptotic equivalence of the grids for different coefficients $\sigma \in \mathcal{S}$ (statement (b)) has been observed in all our numerical experiments. In section 5, we show that this is true if all $\sigma \in \mathcal{S}$ are $C^{1,1}(0, L)$ functions and if $\mathcal{L}_k$ contains high-frequency spectral points λ (this is where the problem is most singular). The complete proof of statement (b) is work in progress.

In many problems, some prior knowledge of unknown σ is available, and we can let $\mathcal{S}$ be the set of functions $\sigma(z)$ that are close to a given $\sigma^{(0)}(z)$. Here, we consider such a set-up,

where $\sigma^{(0)}(z) \equiv 1$ and $\mathcal{S}$, which contains $\sigma^{(0)}$, is a set of sufficiently smooth, positive functions $\sigma(z)$. We solve the discrete inverse problem on our set $\mathcal{S}$, by choosing the optimal grid

$$\mathcal{G}_k^{\sigma^{(0)}} = \{z_i^{\sigma^{(0)}}, 1 \leqslant i \leqslant k+1 \text{ and } \hat{z}_i^{\sigma^{(0)}}, 0 \leqslant i \leqslant k\},$$

defined for $\sigma^{(0)} \equiv 1$. Then, given this grid and the $2k$ coefficients γ_i, $\hat{\gamma}_i$, which are solutions of (4.39), we find $\{\sigma_i\}_{i=1}^{k+1}$ and $\{\hat{\sigma}_i\}_{i=0}^{k}$ from (2.10). The following proposition shows that the optimal grid provides the necessary conditions for convergence of the discrete inverse solution to the true solution.

Proposition 4. *Let γ_j and $\hat{\gamma}_j$, for $1 \leqslant j \leqslant k$, be obtained from the inverse problem (4.39) for $\sigma(z) \in \mathcal{S}$. Then, for any grid (i.e. nonoptimal) with primary nodes z_j, $j = 1, \ldots, k+1$ and dual nodes $\hat{z}_i$, $i = 0, \ldots, k$,*

$$\max_{\sigma \in \mathcal{S}} \left| \int_0^{\hat{z}_i} \sigma(z)\, \mathrm{d}z - \sum_{j=1}^{i} \hat{\gamma}_j \right| \geqslant |\hat{z}_i^{\sigma^{(0)}} - \hat{z}_i|, \qquad i = 1, \ldots, k+1,$$

$$\max_{\sigma \in \mathcal{S}} \left| \int_0^{z_{i+1}} \frac{1}{\sigma(z)}\, \mathrm{d}z - \sum_{j=1}^{i} \gamma_j \right| \geqslant |z_{i+1}^{\sigma^{(0)}} - z_{i+1}|, \qquad i = 1, \ldots, k. \tag{4.41}$$

Proof. By the definition of the optimal grid, γ_j and $\hat{\gamma}_j$, for $1 \leqslant j \leqslant k$, corresponding to $\sigma = \sigma^{(0)} \equiv 1$ satisfy (4.40) with $\epsilon_k = 0$, so with $\sigma \equiv 1$ formulae (4.41) become equalities.

This proposition shows that the convergence of the discrete inverse problem requires grids which are close to the optimal grid for $\sigma^{(0)}$. This condition is, of course, due to the weak dependence of the grid on the particular elements σ in the set $\mathcal{S}$. Note however that the grid depends strongly on the spectral parameters so it is essential that we calculate $\{z_i^{\sigma^{(0)}}\}_{i=1}^{k+1}$, $\{\hat{z}_i^{\sigma^{(0)}}\}_{i=1}^{k}$ such that

$$f_k^{\sigma^{(0)}}(\lambda_i^k) = f^{\sigma^{(0)}}(\lambda_i^k), \qquad \text{for } i = 1, 2 \ldots 2k,$$

where λ_i^k are the same spectral points as in (4.39). □

Numerical experiments using the Padé–Chebyshev numerical code written by Knizhnerman [11] demonstrate the convergence of the solution of the discrete inverse problem to the continuum counterpart. The convergence rate is dependent on the smoothness of the true σ, and our experiments show that it can be very fast. For example, in figure 2, we give the solution of discrete inversion, for a Gaussian σ. We note that, for $k = 10$, the discrete solution is essentially equal to the true σ. In the case of a discontinuous σ (see figure 3), the discrete solution approximates well the true σ, except for Gibbs-like oscillations at the discontinuities. This indicates that the convergence to the true solution is not pointwise but in the weak sense of (4.40).

To illustrate the importance of choosing the correct grid, we show in figure 4 the solution of the same problem as in figure 2, which is obtained on an equidistant grid (conventionally used in the literature on inverse spectral problems [19]). The discrete solution diverges due to false anisotropy, i.e., noncoinciding curves of $\hat{\sigma}_i$ and σ_i at the primary and dual points, respectively. Because of this problem, the conventional approaches require regularization. In fact, our approach is implicitly regularizing and the reconstructions tend to be smooth. However, this regularization is very different from typical approaches which use penalty parameters that are most often ambiguously defined.

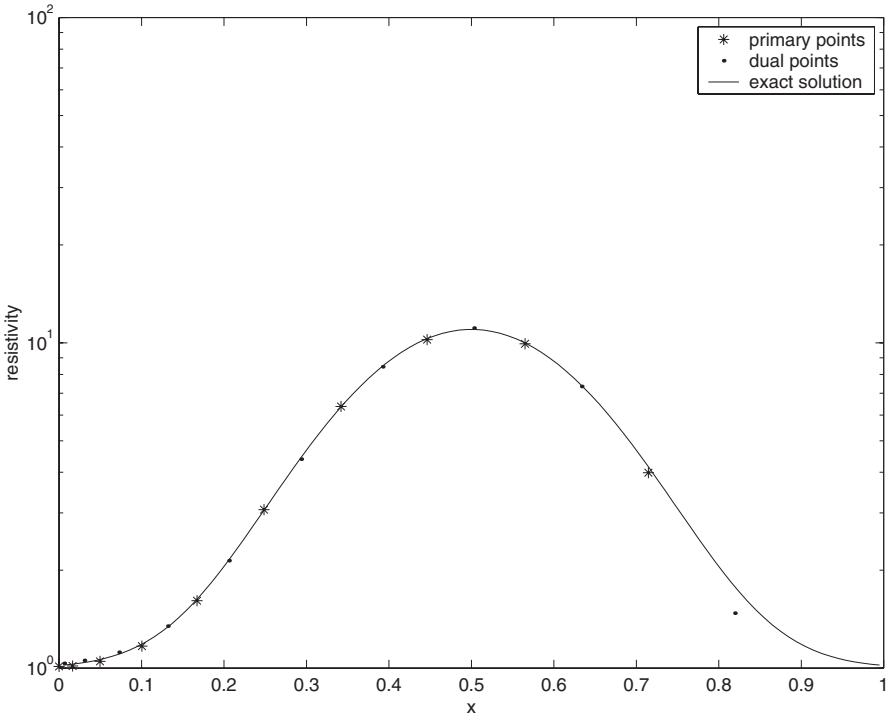

Figure 2. Inversion for Gaussian distribution of σ on an optimal grid with $k = 10$.

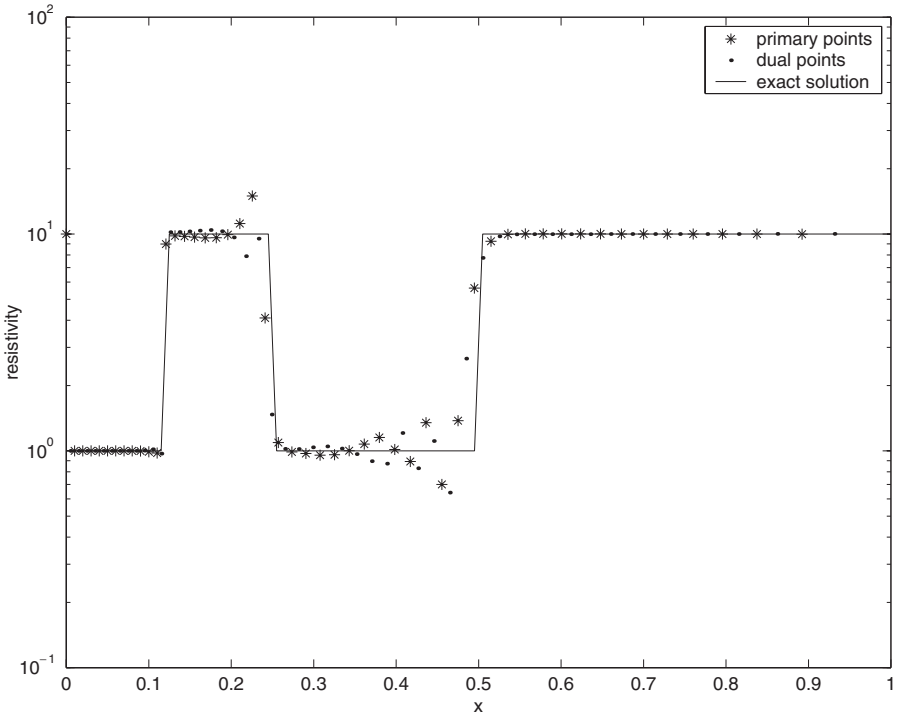

Figure 3. Inversion for discontinuous σ on an optimal grid with $k = 50$.

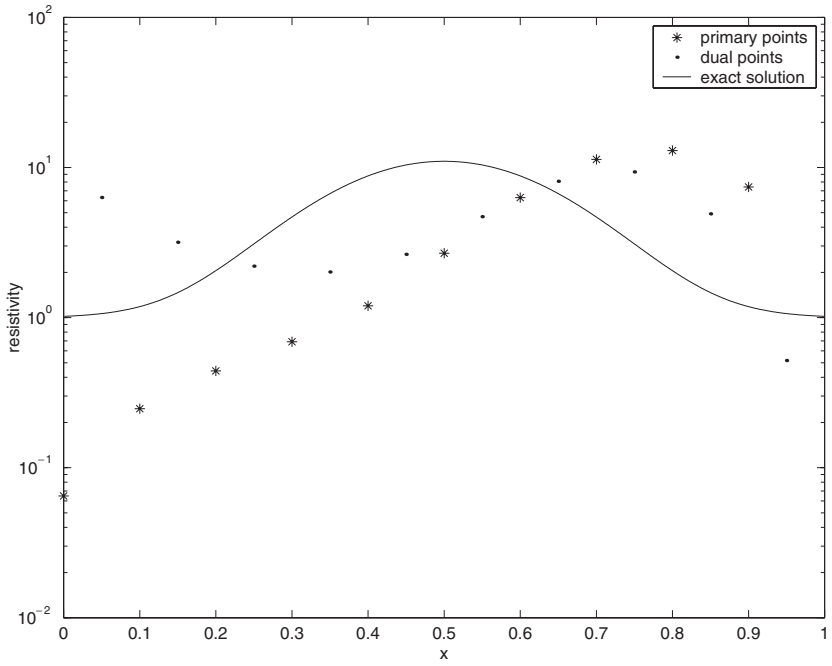

Figure 4. Inversion for Gaussian distribution of σ, $k = 10$, equidistant grid.

5. Analysis of the finite difference solution on optimal grids

In this section, we study in detail the solution of discrete problem (2.8) or, equivalently, (2.12), where the discretization is done on the optimal grid constructed as described in section 2. We focus attention on the case of large spectral parameters λ, where the solution of the resulting Schrödinger equation is approximately equal to the solution of (1.5) with constant σ. Therefore, at least for large $|\lambda|$, we can solve the variable coefficient problem (2.8) on grid $\mathcal{G}_k^{\sigma^{(0)}}$ calculated for constant $\sigma^{(0)}$. Note that, at large $|\lambda|$, the solutions of (1.5) are most singular and therefore very difficult to approximate on a grid. By choosing the optimal grid $\mathcal{G}_k^{\sigma^{(0)}}$, we guarantee exponential accuracy of impedance f_k^{σ} of such singular solutions. At small $|\lambda|$, the solution of (1.5) is smooth and therefore easy to approximate on any grid.

5.1. The Schrödinger equation

We begin our analysis by transforming (1.5) and (2.8) into Schrödinger equations with potential depending on $\sigma(z)$. Assuming that $\sigma(z) \in C^{1,1}(0, L)$, we change variables

$$v(z) = \sqrt{\sigma(z)}\, u(z), \tag{5.1}$$

and rewrite (1.5) as [21, 25, 26]

$$\begin{aligned} &\frac{\mathrm{d}^2 v(z)}{\mathrm{d}z^2} - (q(z) + \lambda) v(z) = 0, \qquad 0 < z < L, \\ &-\frac{\mathrm{d}v(0)}{\mathrm{d}z} + \frac{v(0)}{\sqrt{\sigma(0)}} \frac{\mathrm{d}\sqrt{\sigma}}{\mathrm{d}z}(0) = \frac{1}{\sqrt{\sigma(0)}}, \\ &v(L) = 0, \end{aligned} \tag{5.2}$$

where

$$q(z) = \frac{1}{\sqrt{\sigma(z)}} \frac{\mathrm{d}^2 \sqrt{\sigma(z)}}{\mathrm{d}z^2} \in L^\infty((0, L)) \tag{5.3}$$

is the Schrödinger potential.

In the case of constant $\sigma(z) = \sigma^{(0)} = \sigma(0)$, the Schrödinger potential $q(z)$ vanishes for all $z \in (0, L)$. The solution of (5.2) is

$$w(z) = \frac{1}{\sqrt{\sigma(0)\,\lambda}} \left(\frac{\mathrm{e}^{-\sqrt{\lambda} z} - \mathrm{e}^{\sqrt{\lambda}(z-2L)}}{1 + \mathrm{e}^{-2\sqrt{\lambda} L}} \right) \tag{5.4}$$

and the impedance is given by

$$f^{\sigma^{(0)}}(\lambda) = w(0) = \frac{1}{\sqrt{\sigma^{(0)}\,\lambda}} \left(\frac{1 - \mathrm{e}^{-2\sqrt{\lambda} L}}{1 + \mathrm{e}^{-2\sqrt{\lambda} L}} \right). \tag{5.5}$$

For variable σ and for spectral parameters $|\lambda| \gg 1$, we seek the solution of (5.2), as the WKB asymptotic expansion

$$v(z; \lambda) = \sum_{p=0}^{\infty} \left(\frac{1}{\sqrt{\lambda}} \right)^p g_p(z) \mathrm{e}^{\sqrt{\lambda} s(z)}, \tag{5.6}$$

where $s(z)$, $g_p(z)$ are smooth, O(1) functions. Function $s(z)$ in the exponent of (5.6) satisfies the eikonal equation

$$(s'(z))^2 = 1, \qquad \text{or} \qquad s(z) = \pm z. \tag{5.7}$$

Functions $g_p(z)$, for $p = 0, 1, 2 \ldots$, are determined by solving equation (5.2) to all orders of $\sqrt{\lambda}$ and by imposing the boundary conditions. After a quite standard analysis, we obtain

$$\begin{aligned} v(z; \lambda) = {} & \frac{\mathrm{e}^{-\sqrt{\lambda} z}}{\sqrt{\lambda}\,\sigma(0)(1 + \mathrm{e}^{-2\sqrt{\lambda} L})} \left\{ 1 - \frac{1}{\sqrt{\lambda}} \left[\frac{(1 - \mathrm{e}^{-2\sqrt{\lambda} L}) \ln' \sigma(0) - \mathrm{e}^{-2\sqrt{\lambda} L} \int_0^L q(t)\,\mathrm{d}t}{1 + \mathrm{e}^{-2\sqrt{\lambda} L}} \right.\right. \\ & \left.\left. + \frac{1}{2} \int_0^z q(t)\,\mathrm{d}t \right] + \mathrm{O}\big(|\lambda|^{-\frac{1}{2}}\big) \right\} \\ & - \frac{\mathrm{e}^{\sqrt{\lambda}(z-2L)}}{\sqrt{\lambda}\,\sigma(0)(1 + \mathrm{e}^{-2\sqrt{\lambda} L})} \left\{ 1 - \frac{1}{\sqrt{\lambda}} \left[\frac{(1 - \mathrm{e}^{-2\sqrt{\lambda} L}) \ln' \sigma(0) + \int_0^L q(t)\mathrm{d}t}{1 + \mathrm{e}^{-2\sqrt{\lambda} L}} \right.\right. \\ & \left.\left. - \frac{1}{2} \int_0^z q(t)\mathrm{d}t \right] + \mathrm{O}\big(|\lambda|^{-\frac{1}{2}}\big) \right\} \end{aligned}$$

and, recalling equation (5.4), we have

$$v(z; \lambda) = w(z; \lambda)\big(1 + \mathrm{O}\big(|\lambda|^{-\frac{1}{2}}\big)\big). \tag{5.8}$$

5.2. The discrete Schrödinger equation

To obtain a discrete equivalent of the Schrödinger equation (5.2), we change the variables in (2.8) as

$$V_j = \sqrt{\sigma_j}\, U_j, \qquad \text{for } j = 1, 2 \ldots k+1. \tag{5.9}$$

The transformed finite difference problem is

$$\begin{aligned} & [(V_z)_{\hat{z}}]_j - (Q_j + \lambda) V_j + [(\hat{\beta} V_z)_{\hat{z}}]_j = 0, \qquad j = 1, 2 \ldots k, \\ & - \frac{V_1 - V_0}{h_0} + \frac{V_1}{\sqrt{\sigma_1}} \left(\frac{\sqrt{\sigma_1} - \sqrt{\sigma_0}}{h_0} \right) = \sqrt{\frac{\sigma_0}{\sigma_1}} \frac{1}{\sqrt{\sigma_1}}, \\ & V_{k+1} = 0, \end{aligned} \tag{5.10}$$

where, for $j = 1, 2 \dots k$,

$$Q_j = -\frac{1}{\sqrt{\sigma_j}\,\hat{h}_j}\left(\hat{\sigma}_j \frac{\frac{1}{\sqrt{\sigma_{j+1}}} - \frac{1}{\sqrt{\sigma_j}}}{h_j} - \hat{\sigma}_{j-1}\frac{\frac{1}{\sqrt{\sigma_j}} - \frac{1}{\sqrt{\sigma_{j-1}}}}{h_{j-1}}\right), \tag{5.11}$$

$$\hat{\beta}_j = \frac{\hat{\sigma_j}}{\sqrt{\sigma_j\,\sigma_{j+1}}} - 1, \tag{5.12}$$

$$\left[(V_z)_{\hat{z}}\right]_j = \frac{1}{\hat{h}_j}\left(\frac{V_{j+1} - V_j}{h_j} - \frac{V_j - V_{j-1}}{h_{j-1}}\right), \tag{5.13}$$

$$\left[(\hat{\beta}V_z)_{\hat{z}}\right]_j = \frac{1}{\hat{h}_j}\left(\hat{\beta}_j\frac{V_{j+1} - V_j}{h_j} - \hat{\beta}_{j-1}\frac{V_j - V_{j-1}}{h_{j-1}}\right), \tag{5.14}$$

and where $\sigma(z)$ is extended to the value σ_0, at the dummy node $z_0 < z_1$ introduced in (2.11), such that

$$\frac{\mathrm{d}\sqrt{\sigma}}{\mathrm{d}z}(0) = \frac{\sqrt{\sigma_1} - \sqrt{\sigma_0}}{h_0}. \tag{5.15}$$

5.2.1. Analysis of the error of the discrete impedance. In this section, we estimate the error

$$f_k^{\sigma}(\lambda) - f^{\sigma}(\lambda) = \frac{1}{\sqrt{\sigma(0)}}(V_1 - v(0)),$$

of discrete problem (5.10), for $|\lambda| \gg 1$, on a given, fixed grid with number of points k sufficiently large such that the maximum mesh size

$$h = \max_{j=1,\dots,k} \max(h_k, \tilde{h}_k)$$

satisfies $|\sqrt{\lambda}|h \ll 1$. We also assume that λ does not belong to the spectrum of the discrete operator in (5.10), so the interior error estimate (3.38) holds.

On the same grid, we denote by W_j, for $j = 1, 2 \dots k+1$, the solution of discrete problem

$$\begin{aligned} &[(W_z)_{\hat{z}}]_j - \lambda W_j = 0, \qquad j = 1, 2 \dots k, \\ &-\frac{W_1 - W_0}{h_0} = \frac{1}{\sqrt{\sigma(0)}}, \\ &W_{k+1} = 0, \end{aligned} \tag{5.16}$$

corresponding to a constant $\sigma = \sigma(0) = \sigma_1$. Let us multiply the first equation in (5.10) by $\hat{h}_j W_j$ and sum over j to obtain

$$\begin{aligned} \sum_{j=1}^{k}\Bigg[W_j\left(\frac{V_{j+1} - V_j}{h_j} - \frac{V_j - V_{j-1}}{h_{j-1}}\right) - (\lambda + Q_j)\hat{h}_j V_j W_j \\ + W_j\left(\hat{\beta}_j\frac{V_{j+1} - V_j}{h_j} - \hat{\beta}_{j-1}\frac{V_j - V_{j-1}}{h_{j-1}}\right)\Bigg] = 0 \end{aligned}$$

or, equivalently, by summation by parts,

$$\begin{aligned} \sum_{j=1}^{k}\Bigg[V_j\left(\frac{W_{j+1} - W_j}{h_j} - \frac{W_j - W_{j-1}}{h_{j-1}} - \lambda\hat{h}_j W_j\right) - \hat{h}_j Q_j V_j W_j \\ - h_j\hat{\beta}_j\left(\frac{W_{j+1} - W_j}{h_j}\right)\left(\frac{V_{j+1} - V_j}{h_j}\right)\Bigg] \\ = \frac{V_1 W_0}{h_0} - \frac{V_0 W_1}{h_0} - \hat{\beta}_0 W_1\left(\frac{V_1 - V_0}{h_0}\right). \end{aligned}$$

Note that

$$\frac{V_1W_0}{h_0} - \frac{V_0W_1}{h_0} = -V_1\left(\frac{W_1 - W_0}{h_0}\right) + W_1\left(\frac{V_1 - V_0}{h_0}\right)$$

and, due to (5.16) and the boundary conditions in (5.10), we have

$$\frac{V_1 - W_1}{\sqrt{\sigma(0)}} = -\sum_{j=1}^{k}\left[\hat{h}_j Q_j V_j W_j + h_j\hat{\beta}_j\left(\frac{W_{j+1} - W_j}{h_j}\right)\left(\frac{V_{j+1} - V_j}{h_j}\right)\right] - \frac{V_1W_1}{\sqrt{\sigma(0)}}\frac{\mathrm{d}\sqrt{\sigma}}{\mathrm{d}z}(0)$$
$$+ \frac{W_1}{\sqrt{\sigma(0)}}\left(\sqrt{\frac{\sigma_0}{\sigma_1}} - 1\right) + \hat{\beta}_0\frac{W_1}{\sqrt{\sigma(0)}}\left(\sqrt{\frac{\sigma_0}{\sigma_1}} - V_1\frac{\mathrm{d}\sqrt{\sigma}}{\mathrm{d}z}(0)\right). \tag{5.17}$$

Moreover, a similar calculation for the continuum equation (5.2) gives

$$\frac{v(0) - w(0)}{\sqrt{\sigma(0)}} = -\int_0^L q(z)w(z)v(z)\,\mathrm{d}z - \frac{w(0)v(0)}{\sqrt{\sigma(0)}}\frac{\mathrm{d}\sqrt{\sigma}}{\mathrm{d}z}(0). \tag{5.18}$$

At each grid point z_j, we define errors

$$E_j^V = V_j - v(z_j), \qquad E_j^W = W_j - w(z_j), \tag{5.19}$$

corresponding to finite difference equations (5.10) and (5.16), respectively and, using equations (5.17) and (5.18), we obtain

$$\frac{E_1^V - E_1^W}{\sqrt{\sigma(0)}} = \frac{W_1}{\sqrt{\sigma(0)}}\left(\sqrt{\frac{\sigma_0}{\sigma_1}} - 1\right) + \frac{\hat{\beta}_0W_1}{\sqrt{\sigma(0)}}\left(\sqrt{\frac{\sigma_0}{\sigma_1}} - V_1\frac{\mathrm{d}\sqrt{\sigma}}{\mathrm{d}z}(0)\right)$$
$$- \left(\frac{w(0)E_1^V + v(0)E_1^W + E_1^VE_1^W}{\sqrt{\sigma(0)}}\right)\frac{\mathrm{d}\sqrt{\sigma}}{\mathrm{d}z}(0)$$
$$+ \left[\int_0^L q(z)v(z)w(z)\,\mathrm{d}z - \sum_{j=1}^{k}\hat{h}_jQ_jV_jW_j\right]$$
$$- \sum_{j=1}^{k}h_j\hat{\beta}_j\left(\frac{W_{j+1} - W_j}{h_j}\right)\left(\frac{V_{j+1} - V_j}{h_j}\right). \tag{5.20}$$

The first term in (5.20) is

$$\mathcal{T}_1 = \frac{W_1}{\sqrt{\sigma(0)}}\left(\sqrt{\frac{\sigma_0}{\sigma_1}} - 1\right) = -h_0(w(0) + E_1^W)\frac{\mathrm{d}\sqrt{\sigma}}{\mathrm{d}z}(0) = \mathrm{O}\left(\frac{h_0}{\sqrt{|\lambda|}} + h_0E_1^W\right) \tag{5.21}$$

and it can be made arbitrarily small by choosing dummy node z_0 arbitrarily close to z_1, such that $h_0 \to 0$. Similarly, the second term in (5.20),

$$\mathcal{T}_2 = \frac{\hat{\beta}_0W_1}{\sqrt{\sigma(0)}}\left(\sqrt{\frac{\sigma_0}{\sigma_1}} - V_1\frac{\mathrm{d}\sqrt{\sigma}}{\mathrm{d}z}(0)\right), \tag{5.22}$$

where

$$\hat{\beta}_0 = \frac{\hat{\sigma}_0}{\sqrt{\sigma_0\sigma_1}} - 1 = \sqrt{\frac{\sigma_1}{\sigma_0}} - 1 = \frac{h_0}{\sqrt{\sigma_0}}\frac{\mathrm{d}\sqrt{\sigma}}{\mathrm{d}z}(0),$$

can be made arbitrarily small. The third term in (5.20) is

$$\mathcal{T}_3 = \left(\frac{w(0)E_1^V + v(0)E_1^W + E_1^VE_1^W}{\sqrt{\sigma(0)}}\right)\frac{\mathrm{d}\sqrt{\sigma}}{\mathrm{d}z}(0) = \mathrm{O}\left(\frac{E_1^V + E_1^W}{\sqrt{|\lambda|}}\right), \tag{5.23}$$

where we use (5.4), (5.8) and where we neglect the quadratic term in the error.

We rewrite the fourth term in (5.20) as

$$\mathcal{T}_4 = \left[\int_0^L q(z)v(z)w(z)\,\mathrm{d}z - \sum_{j=1}^{k}\hat{h}_j q(z_j)v(z_j)w(z_j)\right] - \sum_{j=1}^{k}\hat{h}_j E_j^Q v(z_j)w(z_j)$$
$$- \sum_{j=1}^{k}\hat{h}_j Q(z_j)(E_j^V w(z_j) + E_j^W v(z_j) + E_j^W E_j^V), \tag{5.24}$$

where $E_j^Q = Q_j - q(z_j)$. The first part of $\mathcal{T}_4$ is quadrature error, where we approximate the integrand by a piecewise constant function defined on the grid, which we assume satisfies property (2.30). By (5.4) and (5.8), the first and second derivatives of the integrand are $\mathrm{O}(\frac{1}{\sqrt{|\lambda|}})$ and $\mathrm{O}(1)$, respectively, so the quadrature error is $\mathrm{O}(h^2 + \frac{h}{\sqrt{|\lambda|}})$. We also have

$$\left|\sum_{j=1}^{k}\hat{h}_j E_j^Q v(z_j)w(z_j)\right| \leqslant \|wv\|_{L^\infty[0,L]}\sum_{j=1}^{k}\hat{h}_j|E_j^Q| = \|wv\|_{L^\infty[0,L]}\|E^Q\|_1 = \mathrm{O}\left(\frac{\|E^Q\|_1}{|\lambda|}\right),$$
$$\left|\sum_{j=1}^{k}\hat{h}_j q(z_j)v(z_j)E_j^W\right| \leqslant \|qv\|_{L^\infty[0,L]}\sum_{j=1}^{k}\hat{h}_j|E_j^W| = \|qv\|_{L^\infty[0,L]}\|E^W\|_1 = \mathrm{O}\left(\frac{\|E^W\|_1}{\sqrt{|\lambda|}}\right)$$

and

$$\left|\sum_{j=1}^{k}\hat{h}_j q(z_j)w(z_j)E_j^V\right| \leqslant \|qv\|_{L^\infty[0,L]}\sum_{j=1}^{k}\hat{h}_j|E_j^W| = \|qw\|_{L^\infty[0,L]}\|E^V\|_1 = \mathrm{O}\left(\frac{\|E^V\|_1}{\sqrt{|\lambda|}}\right).$$

Therefore, neglecting quadratic terms in the error,

$$\mathcal{T}_4 = \mathrm{O}\left(h^2 + \frac{h}{\sqrt{|\lambda|}}\right) + \mathrm{O}\left(\frac{\|E^V\|_1 + \|E^W\|_1}{\sqrt{|\lambda|}}\right).$$

Finally, we note that error estimate (3.38) applied to the homogeneous problem, with truncation error (see equation (3.35))

$$T_j = \mathrm{O}\left(\sqrt{|\lambda|}\left(\frac{h_j + h_{j-1}}{2\hat{h}_j} - 1\right) + |\lambda|\left(\frac{h_j^2 - h_{j-1}^2}{6\hat{h}_j}\right)\right),$$

gives $\frac{\|E^V\|_1}{\sqrt{|\lambda|}} \gg \mathrm{O}\big(h^2 + \frac{h}{\sqrt{|\lambda|}}\big)$ so the fourth term in (5.20) is

$$\mathcal{T}_4 = \mathrm{O}\left(\frac{\|E^V\|_1 + \|E^W\|_1}{\sqrt{|\lambda|}}\right). \tag{5.25}$$

The last term in (5.20) is

$$\mathcal{T}_5 = \sum_{j=1}^{k} h_j\hat{\beta}_j\left(\frac{W_{j+1} - W_j}{h_j}\right)\left(\frac{V_{j+1} - V_j}{h_j}\right). \tag{5.26}$$

We define

$$\hat{G}_i = \sum_{j=1}^{i} h_{j-1}\left(\frac{W_j - W_{j-1}}{h_{j-1}}\right)\left(\frac{V_j - V_{j-1}}{h_{j-1}}\right)$$
$$= \sum_{j=1}^{i} h_{j-1}\left(\frac{w(z_j) - w(z_{j-1})}{h_{j-1}}\right)\left(\frac{v(z_j) - v(z_{j-1})}{h_{j-1}}\right)$$
$$+ \sum_{j=1}^{i} h_{j-1}\left(\frac{w(z_j) - w(z_{j-1})}{h_{j-1}}\right)\left(\frac{E_j^V - E_{j-1}^V}{h_{j-1}}\right)$$

$$+\sum_{j=1}^{i} h_{j-1}\left(\frac{E_j^W - E_{j-1}^W}{h_{j-1}}\right)\left(\frac{v(z_j)-v(z_{j-1})}{h_{j-1}}\right)$$
$$+\sum_{j=1}^{i} h_{j-1}\left(\frac{E_j^W - E_{j-1}^W}{h_{j-1}}\right)\left(\frac{E_j^V - E_{j-1}^V}{h_{j-1}}\right) \tag{5.27}$$

and obtain by summation by parts

$$\sum_{j=1}^{k} h_j\hat{\beta}_j\left(\frac{W_{j+1}-W_j}{h_j}\right)\left(\frac{V_{j+1}-V_j}{h_j}\right) = -\sum_{j=1}^{k}\hat{h}_j\left(\frac{\hat{\beta}_j-\hat{\beta}_{j-1}}{\hat{h}_j}\right)\hat{G}_j - \hat{\beta}_0\hat{G}_1 + \hat{\beta}_k\hat{G}_{k+1}. \tag{5.28}$$

The first term in (5.27) is

$$\sum_{j=1}^{i} h_{j-1}\left(\frac{w(z_j)-w(z_{j-1})}{h_{j-1}}\right)\left(\frac{v(z_j)-v(z_{j-1})}{h_{j-1}}\right)$$
$$= \int_0^{z_i}\frac{\mathrm{d}w}{\mathrm{d}z}(z)\frac{\mathrm{d}v}{\mathrm{d}z}(z)\,\mathrm{d}z + \mathcal{E}^{\mathrm{qdr}} = \mathrm{O}\left(\frac{1}{\sqrt{|\lambda|}}\right) + \mathcal{E}^{\mathrm{qdr}},$$

where the quadrature error is $\mathcal{E}^{\mathrm{qdr}} = \mathrm{O}\big(\sqrt{|\lambda|}h + |\lambda|h^2\big) \ll 1$, since the first and second derivatives of $\frac{\mathrm{d}w}{\mathrm{d}z}(z)\frac{\mathrm{d}v}{\mathrm{d}z}(z)$ are $\mathrm{O}(\sqrt{|\lambda|})$ and $\mathrm{O}(|\lambda|)$, respectively. Using summation by parts, we rewrite the second term in (5.27) as

$$\sum_{j=1}^{i} h_{j-1}\left(\frac{w(z_j)-w(z_{j-1})}{h_{j-1}}\right)\left(\frac{E_j^V - E_{j-1}^V}{h_{j-1}}\right)$$
$$= -\sum_{j=1}^{i} E_j^V\left(\frac{w(z_{j+1})-w(z_j)}{h_j} - \frac{w(z_j)-w(z_{j-1})}{h_j - 1}\right)$$
$$+ E_i^V\left(\frac{w(z_{i+1})-w(z_i)}{h_i}\right) - E_0^V\left(\frac{w(z_1)-w(z_0)}{h_0}\right).$$

From (3.35), applied to $\sigma \equiv 1$, we have that

$$\sum_{j=1}^{i} E_j^V\left(\frac{w(z_{j+1})-w(z_j)}{h_j} - \frac{w(z_j)-w(z_{j-1})}{h_{j-1}}\right) = \sum_{j=1}^{i}\hat{h}_j E_j^V(T_j + \lambda w(z_j)),$$

where $E_j^V = \mathrm{O}(T_j)$, as given by (3.38). Thus, neglecting quadratic terms in the error and using the maximum norm $\|E^V\|_\infty$, we have

$$\left|\sum_{j=1}^{i} h_{j-1}\left(\frac{w(z_j)-w(z_{j-1})}{h_{j-1}}\right)\left(\frac{E_j^V - E_{j-1}^V}{h_{j-1}}\right)\right| \leqslant |\lambda|\|E^V\|_\infty\int_0^L w(z)\,\mathrm{d}z = \mathrm{O}(\|E^V\|_\infty).$$

A similar estimate holds for the third term in (5.27), so, neglecting quadratic terms in the error, we have

$$|\hat{G}_i| \leqslant \mathrm{O}(\|E^V\|_\infty + \|E^W\|_\infty), \qquad \text{for } i = 0, 1\ldots k+1.$$

Using this bound on $\hat{G}_i$, equation (5.28) gives

$$|\mathcal{T}_5| \leqslant \|\hat{G}\|_\infty\sum_{j=1}^{k}\hat{h}_j\left|\frac{\hat{\beta}_j-\hat{\beta}_{j-1}}{\hat{h}_j}\right| = \mathrm{O}(\|E^V\|_\infty + \|E^W\|_\infty)\mathrm{Var}(\hat{\beta}). \tag{5.29}$$

Finally, we note that

$$\hat{\beta}_j = \frac{\hat{\sigma}_j}{\sqrt{\sigma_j\sigma_{j+1}}} - 1 = \mathrm{O}\left(\hat{z}_j - z_j - \frac{h_j}{2}\right) \leqslant T_j$$

so, the variation of β is at most as large as the truncation error. Equivalently, by (3.38), $\mathrm{Var}(\hat{\beta}) \leqslant \mathrm{O}(\|E^V\|_\infty)$, which means that $\mathcal{T}_5$ is quadratic in the error.

Gathering all the results above, we have that

$$f_k^\sigma(\lambda) - f^\sigma(\lambda) = \frac{E_1^V}{\sqrt{\sigma}_1} = \frac{E_1^W}{\sqrt{\sigma}_1} + \mathrm{O}\left(\frac{\|E^V\|_1 + \|E^W\|_1}{\sqrt{|\lambda|}}\right), \tag{5.30}$$

so, for $|\lambda| \gg 1$, the error in the impedance of discrete problem (5.10), for variable σ, is determined by the error E_1^W in the impedance of the homogeneous problem. By choosing our grid as $\mathcal{G}_k^{\sigma^{(0)}}$, the optimal grid for the homogeneous problem, we ensure therefore that the approximation of impedance $f^\sigma(\lambda)$ is also accurate.

In conclusion, we have shown that optimal grids for constant coefficient problems are asymptotically optimal for direct, variable coefficient problems. This partially explains the experimental observation of section 4 that the grids, which are optimal for different distributions of the coefficients, are asymptotically close to each other for large k. For the rigorous proof of the latter we also need the uniform stability of the discrete inverse problems in appropriate norms. The work on such a stability result is in progress.

6. Conclusions

We have proven that, for the convergence of the one-dimensional discrete inverse problem, it is necessary that the finite difference grid is close enough to the optimal grid for the homogeneous medium. Numerical experiments indicate that optimal grids for different coefficient distributions (but obtained for the same measurement spectral parameters λ_p) are close to the grid for the homogeneous medium, and the latter is sufficient for the convergence of the discrete inverse problem.

We have found that the optimal grids for constant coefficients can be used efficiently for the solution of direct problems with variable coefficients. In fact, this explains partially the efficiency of using such grids in inverse problems. More precisely, we have proven fast convergence of high-frequency asymptotes of impedance functions of variable coefficient problems obtained on optimal grids for constant coefficient problems. The analysis is based on the fact that the Sturm–Liouville equation can be transformed into the Schrödinger equation with leading terms that are the same as in the constant coefficient one-dimensional Helmholtz equation.

The results of this work can be extended to some multi-dimensional problems using tensor products of one-dimensional optimal grids. These problems are limited to those that have constant coefficient Helmholtz equations as the leading part, i.e., Euclidean metrics for high-frequency asymptotes. For example, such problems include the direct current equation considered in section 1.2, with σ depending on two variables. Furthermore, in this case, proposition 4 can be extended to the two-dimensional inverse problem on circular graphs [20] using the tensor product of optimal radial and equidistant angular grids.

A very successful application to the (direct problem) solution of low-frequency Maxwell's equations in three-dimensional, anisotropic, inhomogeneous conductive media is shown in [27]. Unfortunately, it is not clear how to extend the obtained results to multi-dimensional wave problems with variable speed, where the coordinate transform (1.3) generates non-Euclidean metrics.

Acknowledgments

The authors are very grateful to their friends and colleagues: Tarek Habashy for sharing his many insightful ideas; David Ingerman for the ideas of the proofs of propositions 1 and 2;

and Leonid Knizhnerman for the permission to use his optimal grid generator code. We are also very grateful to Professor J B Keller for his very helpful suggestions on improving our explanation.

The work of LB was partially supported by the National Science Foundation under grant number DMS-9971209 and by the Office of Naval Research, under grant N00014-02-1-0088. The work of VD was supported by Schlumberger Technology and partially by Mathematical Science Research Institute Fall 2001 semester on Inverse Problems.

References

[1] Givoli D and Keller J B 1989 Exact nonreflecting boundary conditions *J. Comput. Phys.* **82** 172–92
[2] Grote M J and Keller J B 1995 On nonreflecting boundary conditions *J. Comput. Phys.* **122** 231–43
[3] Glowinski R, Golub G H, Meurant G A and Periaux J (ed) 1990 *Domain Decomposition Methods for Partial Differential Equations* (Philadelphia, PA: SIAM)
[4] Quarteroni A and Valli A 1999 Domain decomposition methods for partial differential equations *Numerical Mathematics and Scientific Computation* (New York: Clarendon)
[5] Gelf'and I M and Levitan B M 1956 On the determination of a differential equation from its spectral function *AMS Transl.* 253–304
[6] Levitan B M 1987 *Inverse Sturm–Liouville Problems* (Utrecht: VNU Science Press)
[7] Chadan K, Colton D, Päivärinta L and Rundell W 1997 *An Introduction to Inverse Scattering and Inverse Spectral Problems* (Philadelphia, PA: SIAM)
[8] Engquist B and Majda A 1977 Absorbing boundary conditions for the numerical simulation of waves *Math. Comput.* **31** 629–51
[9] Trefethen L and Halpern L 1977 Well-posedness of one-way wave equations and absorbing boundary conditions *Math. Comput.* **31** 629–51
[10] Schmitt B A 1992 Krylov approximations for matrix square roots in stiff boundary value problems *Math. Comput.* **58** 191–212
[11] Druskin V and Knizhnerman L 2000 Gaussian spectral rules for three-point second differences: I. A two-point positive definite problem in a semiinfinite domain *SIAM J. Numer. Anal.* **37** 403–22
[12] Ingerman D, Druskin V and Knizhnerman L 2000 Optimal finite-difference grids and rational approximations of the square root: I. Elliptic problems *Commun. Pure Appl. Math.* **53** 1039–66
[13] Baker G A and Graves-Morris P 1996 *Padé Approximants* (London: Addison-Wesley)
[14] Iserles A and Strang G 1983 The optimal accuracy of difference schemes *Trans. Am. Math. Soc.* **277** 779–803
[15] Mackenzie J A 1998 The efficient generation of simple two-dimensional adaptive grids *SIAM J. Sci. Comput.* **19** 1340–65
[16] Druskin V and Moskow S 2001 Three-point finite difference schemes. Padé and the spectral Galerkin method: I. One-sided impedance approximation *J. Math. Comput.*
[17] Druskin V and Knizhnerman L 2000 Gaussian spectral rules for second order finite-difference schemes *Numer. Algorithms* **25** 139–59
[18] Asvadurov S, Druskin V and Knizhnerman L 2000 Application of the difference Gaussian rules to solution of hyperbolic problems *J. Comput. Phys.* **158** 116–35
[19] Chu M T and Golub G H 2001 Structured inverse eigenvalue problems *Acta Numer.* 1–70
[20] Ingerman D and Morrow J 1998 On a characterization of the kernel of the Dirichlet-to-Neumann map for a planar region *SIAM J. Math. Anal.* **29** 106–15
[21] Uhlmann G 1999 Developments in inverse problems since Calderón's foundational paper *Harmonic Analysis and Partial Differential Equations (Chicago Lectures in Mathematics)* pp 295–345
[22] Nikishin E M and Sorokin V N 1991 *Rational Approximations and Orthogonality (Transl. Mathematical Monographs vol 92)* (Providence, RI: American Mathematical Society)
[23] Kac I S and Krein M G 1974 On the spectral functions of the string *Am. Math. Soc. Transl., Ser. 2* **103** 19–102
[24] Rudin W 1976 *Principles of Mathematical Analysis* 3rd edn (New York: McGraw-Hill)
[25] Sylvester J and Uhlmann G 1987 A global uniqueness theorem for an inverse boundary value problem *Ann. Math.* **125** 153–69
[26] Nachman A I 1988 Reconstructions from boundary measurements *Ann. Math.* **128** 531–76
[27] Davydycheva S, Druskin V and Habashy T An efficient finite-difference scheme for electromagnetic logging in 3-d anisotropic inhomogeneous media *Geophysics* submitted